Microfluidic 3D cell culture for high throughput screening

Trietsch, S.J.

Chapter 5

Membrane-free culture and real-time barrier integrity assessment of perfused intestinal epithelium tubes

SJ Trietsch, E Naumovska, D Kurek, MC Setyawati, MK Vormann, KJ Wilschut, HL Lanz, A Nicolas, CP Ng, J Joore, S Kustermann, A Roth, T Hankemeier, A Moisan, P Vulto*

Nature Communications

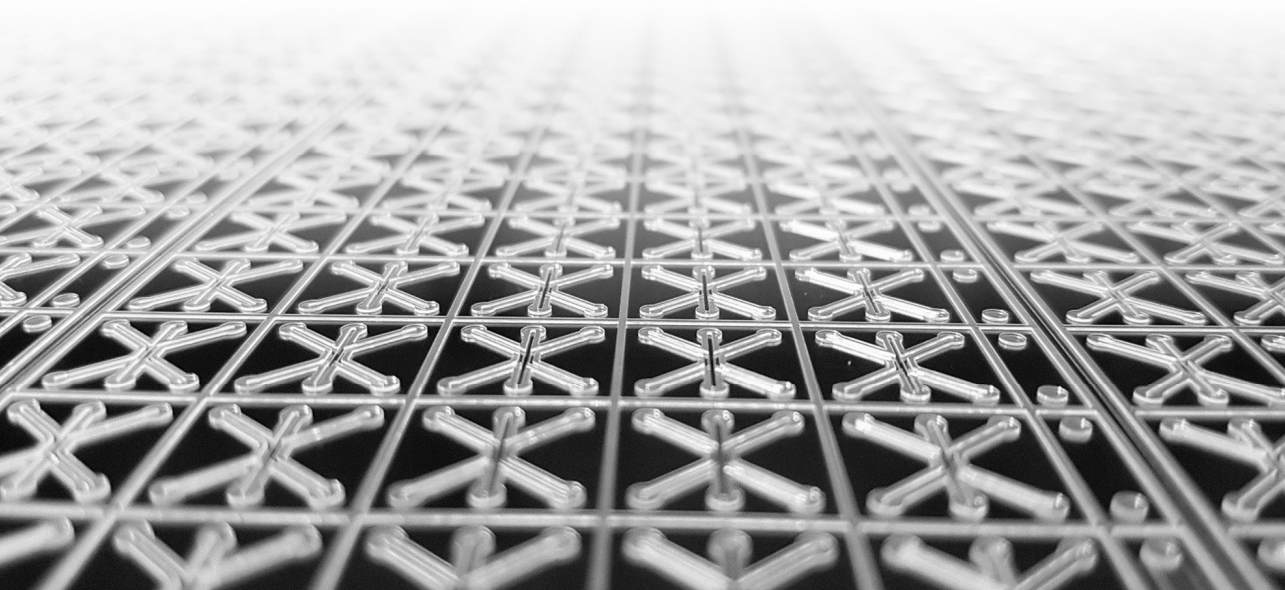

Abstract

In vitro models that better reflect in vivo epithelial barrier (patho-)physiology are urgently required to predict adverse drug effects. Here we introduce extracellular matrix-supported intestinal tubules in perfused microfluidic devices, exhibiting tissue polarization and transporter expression. Forty leak tight tubules are cultured in parallel on a single plate and their response to pharmacological stimuli is recorded over 125 hours using automated imaging techniques. A study comprising 357 gut tubes is performed of which 93% are leak tight before exposure. EC50-time curves could be extracted that provide insight in both concentration and exposure time response. Full compatibility with standard equipment and user-friendly operation, make this the first Organ-on-a-Chip platform that is readily applicable in routine laboratories.

Introduction

Dysfunction of epithelial barriers as a result of pathological states or drug-induced toxicity can lead to life-threatening conditions and halt drug development at all clinical stages. Epithelial barrier disruption is mainly manifested by an increased para-cellular permeability of the epithelium. *In vitro* testing of para-cellular permeability of epithelial barriers is most commonly achieved by cultivating cells on a rigid membrane that separates two medium-containing chambers under static conditions. Such conventional Transwell systems are poorly suited for high-resolution kinetic measurements and image-based readouts and therefore provide only limited information on the underlying mechanisms leading to barrier disruption. More importantly, it does not comply with the current paradigm in cell culture that is steadily shifting towards three-dimensional cultures , extracellular matrix (ECM) embedment and addition of perfusion flow.[1–5]

The field of microfluidics has rapidly gained momentum in the realm of *in vitro* modelling.[3] Inherent to its dimensions, microfluidic techniques are uniquely suitable to connect with epithelia of tubular shapes in order to provide shear stress and continuous medium refreshment through perfusion. Typical microfluidic solutions make use of artificial membranes to enable apical-basal access to the epithelia[6], thus not accommodating an ECM that is a crucial parameter in cell signaling involved in differentiation and epithelial-to-mesenchymal transition. Also, microfluidic techniques, which are typically presented as single chips[7], need to be parallelized in order to deliver readouts for multiple compounds, dilutions,

replicates and controls. User-friendly operation and compatibility with state-of-the-art readouts, such as high content imaging-based multiplexed cellular and molecular analyses are crucial prerequisites for perfused ECM embedded cell culture techniques to become a new standard.[8]

We developed a methodology to culture perfused, ECM-supported epithelia and interrogate their barrier function in a membrane-free manner. As an example, we developed a model of intestinal tract epithelium that exhibits cellular polarization, tight junction formation and expression of key receptors. Forty gut models were grown in a tubular shape in the OrganoPlate platform that were accessible from both the apical and basal sides. The tubes were assessed for barrier integrity and exposed to staurosporine and acetylsalicylic acid (aspirin) for 125 hours. From 330 tubes used in these experiments, 93% were leak tight before exposure. The experiment was repeated using real-time parallel time-lapse imaging in which tubes were stable up till 6 to 8 hours. EC50-time curves provide insight in concentration response at increasing exposure time in one single experimental run.

Results

Figure 1 shows the OrganoPlate platform, which encompasses 40 microfluidic cell culture structures embedded in a standard 384-well microtiter plate format (Fig. 1a-b).[9,10] Each microfluidic channel structure is comprised of three lanes that are connected to corresponding wells of a microtiter plate that function as inlets and outlets to access the microfluidic culture. The lanes join in the centre of the structure where two capillary pressure barriers are present called phaseguides.[11] Figure 1c-j show a schematic representation of vertical and horizontal cross-sections of the centre of a microfluidic structure and the method of growing a tubular structure. First an ECM gel is introduced in the central lane (Fig. 1c-d). The phaseguides are used to selectively pattern the ECM gel in the central lane by meniscus pinning. The meniscus stretches beyond the phaseguide, leading to a curved shape. After ECM gelation, epithelial cells are seeded in one lateral lane, allowing them to sediment directly against the ECM gel by placing the titre plate in a vertical position, i.e. standing on one side (Fig.1e-h). Upon attachment of the cells, the plate is horizontally placed on an interval rocker that induces flow by reciprocal leveling between reservoirs (SI1). Upon application of flow, cells proliferate and start lining all surfaces of the perfusion channel, forming a confluent tubular structure (Fig. 1i-j). The tubules have a lumen that is connected to the in- and outlet of the respective lane

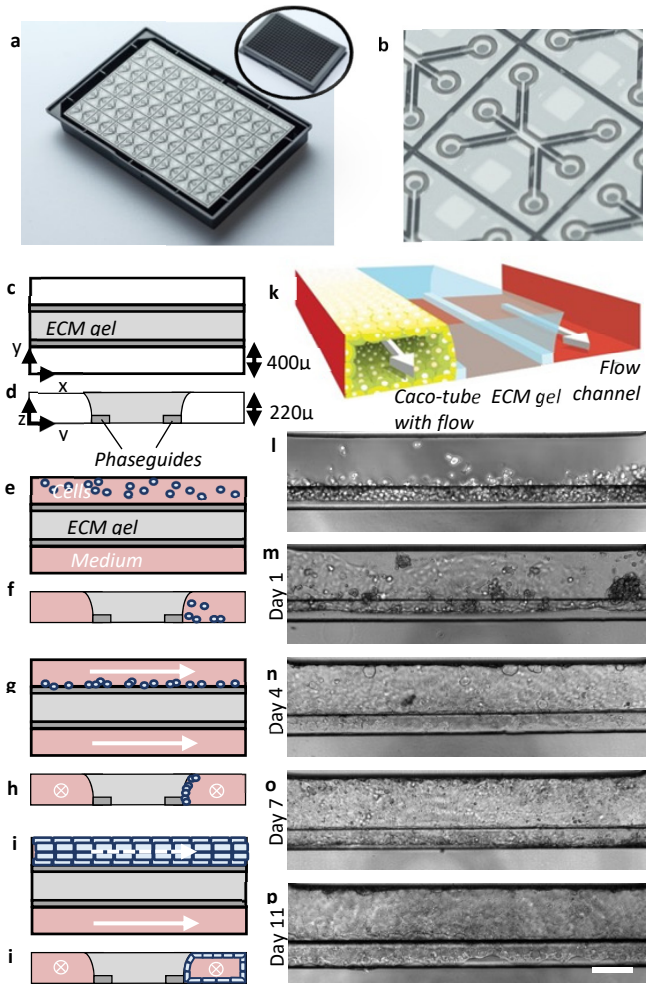

Figure 1 | Overview of the method for modeling intestinal tubules in the OrganoPlate platform. (a) Photograph of the bottom of an OrganoPlate showing 40 microfluidic channel networks with inlay showing the top view of the 384 well plate format device; **(b**) Zoom-in on a single microfluidic channel network comprising three channels that join in the center. (**c, e, g, i)** Horizontal projection and **(d, f, h, j)** vertical cross section of center region for subsequent steps in establishing the gut model: (**c, d)** an extracellular matrix gel (light grey) is patterned by two phaseguides (dark grey); (**e, f)** Culture medium is introduced in the two lanes adjacent to the ECM gel, one of which comprises cells. (**g, h**) Cells are allowed to settle against the ECM gel surface, by placing the plate on its side; (**i, j)** Upon application of flow, cells form a confluent layer lining the channel and gel surfaces, resulting in a tubular shape. (**k)** 3D artist impression of the center of a chip comprising a tubule, an extra cellular matrix gel and a perfusion lane; two phaseguides (white bars) are present that define the three distinct lanes in the central channel. The tubule has a lumen at its apical side that is perfused. (**l-p)** Phase contrast images of the formation of the tubular structure at day 0, 1, 4, 7 and 11 respectively. Scale bars are 100µm

making it accessible for perfusion with medium and for apical compound exposure. The basal side of the epithelium is facing the ECM gel and can be accessed by the second perfusion lane on the opposite side of the ECM gel lane. Fig. 1k depicts an artist impression of the 3D configuration of the tube, showing that the tube is grown directly against the extracellular matrix, without presence of artificial membranes (Fig. 1k).

For modeling of the intestinal barrier, the human intestinal colorectal adenocarcinoma cell line (Caco-2) was used. Figure 1l-p show phase contrast pictures of tube formation at day 0, 1, 4, 7, and 11 respectively. On day 0, cells are seeded against the ECM and start colonizing the glass walls to form a confluent tube (Fig. 1n-p). Perfusion was crucial for tube formation. Tubes were formed in 3 days and optimal barrier function was found at day 4 (SI1).

Differentiation and polarization marker expression

Figure 2a shows a 3D reconstruction of confocal fluorescence micrographs of the gut tube. The tube has a clear lumen and lines the perimeter of the gel and perfusion lane. Caco-2 cells in the confluent tubule display tight junctions and brush border formation as shown by immunofluorescence staining of ZO-1 and Ezrin respectively[12] (Fig. 2a-d, g). Figure 2e shows localization of acetylated tubulin (microtubules) and occludin (tight junctions)[13]. Dome-formation is observed, indicative of active fluid transport and intact epithelial barrier function[14,15] (Fig. 2f). Fig. 2h-j show maximum intensity projection images of tubes stained for Glut-2, MRP2, ErbB1, and ErBb2. Cells in contact with the ECM showed a strongly increased expression of the transporters Glut-2, MRP2 and to a lesser extend ErbB1 and ErbB2 receptors.[16]

These staining results illustrate the crucially instructive role that the extracellular matrix plays in cellular differentiation and protein expression. Furthermore, characteristics of the ECM gel surface, such as its (bio-)chemical composition and mechanical characteristics, allow the formation of tissue structures observed *in vivo*.[17] Polarization of the cell layer against the gel is best visualized at the contact line between the gel meniscus and the phaseguide, at the bending point of the cell layer where apical-basal polarization is in the horizontal plane. This is the most right-hand part of the tube in Fig. 2a or the bottom side of the tube in Fig. 2b. Fig. 2g and SI2 show single z-slices at this bending point, just above the phaseguide.

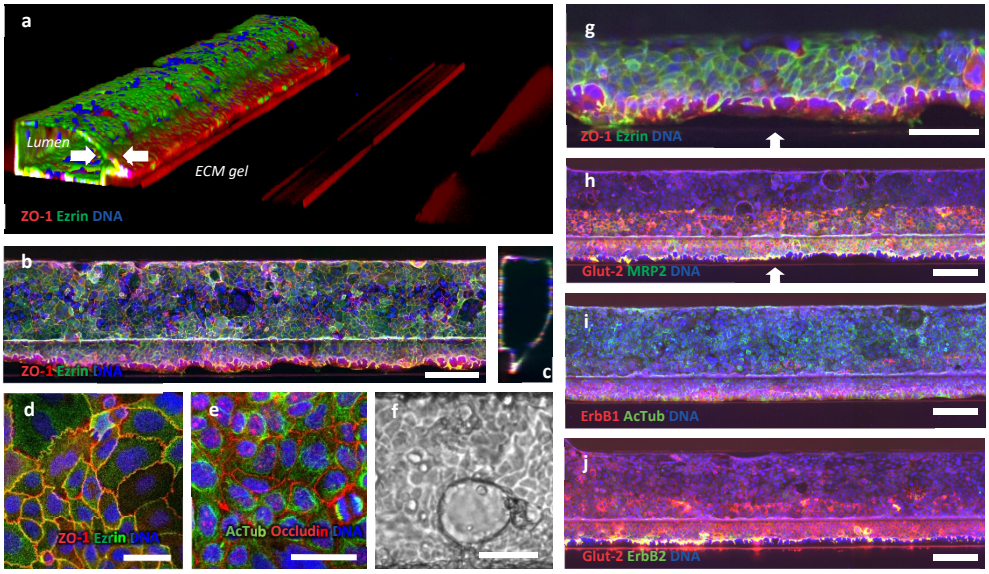

Figure 2 | Tubule characterization by immunofluorescent staining. (a) 3D reconstruction of a confocal z-stack showing tubular morphology with a lumen. White arrows indicate the apical (A) and basal (B) sides. The tube is stained for tight junctions (ZO-1 in red) and brush borders (Ezrin in green). **(b)** max projection and **(c)** vertical cross section of the tubular structure in **(a)**; **(d, e**) Zoom of the epithelial layer at the bottom of the tube exhibiting **(d)**. tight junctions (ZO-1 in red) and brush borders (Ezrin in green) and **(e)** acetylated tubulin (green) and occludin (red). **(f)** Phasecontrast image showing dome formation. **(g)** Zoom of a z-slice of the tube in **(a)** of the cell layer on top of the phaseguide showing apical positioning of Ezrin indicating polarization of the tube (white arrow indicates basal side B). **(h)** expression of glucose and MRP2 transporters respectively stained with Glut-2 in red and MRP2 stain in green. Both Glut-2 and MRP2 show significantly higher signal against the collagen gel compared to the regions that are not exposed to the collagen indicating increased expression levels. Both stains clearly stain the apical side of the tube. For z-slices above the phaseguide at a higher magnification see **SI2b (i)** ErbB1 (red) and acetylated tubulin (green) expression. ErbB1 expression levels appear higher against the collagen. **(j)** Co-staining of Glut-2 transporter and ErbB2 receptor; both stains show higher signal levels against the collagen gel. ErbB2 is primarily expressed pericellularly (see also **SI2d** for a zoom)). All tubes are fixated after four days in culture. Nuclei are stained blue with Draq5 **(a-c, g-j)** and DAPI **(d, e)**. Scale bars in white are 100µm with the exception of **(d, e, f)** and **(g)**, where they are 50µm. Z-slices just above the phaseguide at higher magnification of the images **(g-j)** are available in **SI2**

Tubes are the same as the images of Fig. 2b, h-j, but depicted as single z-slices and at higher magnification. Polarization is confirmed by localization of brush borders (ezrin) and the MRP2 transporter on the apical side as shown in fig. 2g, and SI2a, b, while ErBb2 is positioned pericellularly (see SI2d). At least ten Caco-2 tubes where stained with each marker, figures show a representative selection of results.

Barrier integrity

Barrier function of the Caco-2 tubes was assessed by perfusion with a fluorescent probe in culture medium through the tube lumen, followed by the determination of fluorescence levels in the basal gel region, normalized to the fluorescence in the lumen. This is illustrated in Fig. 3a-i. Both a high molecular weight fluorescent probe (150kDa FITC-dextran) and a lower molecular weight probe (4.4kDa TRITC-dextran) were added to the medium that is perfused through the lumen of the tube. In absence of an intact tubular structure, the fluorescent probes leak into the gel and the basal side perfusion channel (Fig. 3a, d, g), while for a fully intact barrier the fluorescent probes are retained in the lumen of the tube (Fig. 3b, e, h). Upon (partial) loss of barrier function, e.g. through drug-induced toxicity, the fluorescent probe leaks out of the lumen towards the basal side, yielding a higher signal in the ECM (Fig. 3c, f, i). Barrier integrity was measured using a high content imaging (HCI) system allowing monitoring of 40 tubes in parallel. To quantify the integrity of the barrier, the fluorescence level was measured in the gel region and normalized to the fluorescence level in the luminal side to compensate for bleaching effects. Upon reaching a fluorescence value of 0.4, barrier integrity of a tube was considered lost. The barrier integrity of 24 tubes was tracked on day 4, 7 and 11 of culture. As depicted in SI1c, it was found that on day 4 all tubes were leak tight, while at day 7 and 11, three and seven tubes were leaky respectively. Therefore, barrier integrity measurements are performed at 4 days of culture.

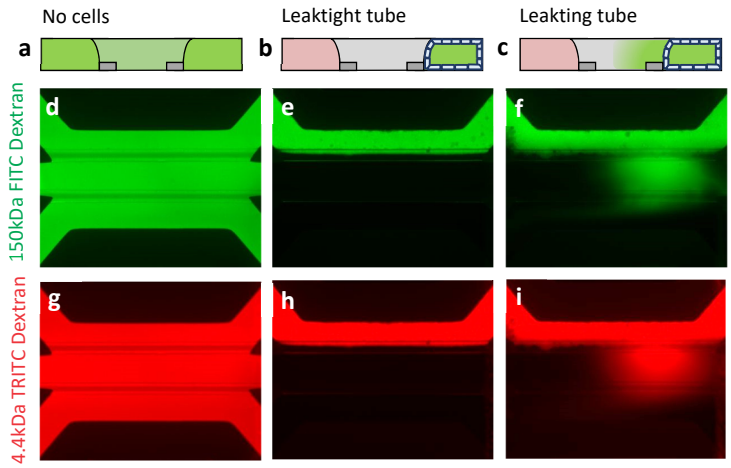

Figure 3 | Barrier integrity assay in OrganoPlate: a fluorescent dye is inserted in the channel comprising the tube. Integrity of the tube barrier is quantified by measuring the amount of dye that is leaking out of the tube into the adjacent gel channel. (a-c) Sketch in vertical cross section showing fluorescence distribution: **(a)** in absence of a tube, **(b)** for the case of a leak tight tube and **(c)** for a leaky tube. **(d-i)** Fluorescent images of microfluidic chips perfused with fluorescent molecules show experimental results for: gel only **(d, g)**, leak-tight tube **(e, h)** and leaky tube **(f-i)** using both a 150kDa FITC-dextran and a 4.4kDa TRITC-Dextran during the same experiment.

Drug induced barrier disruption

Barrier integrity of 4-day-old Caco-2 tubes was assessed during a 125-hour apical exposure to various concentrations of staurosporine (0.4 to 90 μM), an inducer of apoptosis[18] and aspirin which affects tight junctions[19] (0.16 to 40 mM). Fluorescence levels were measured at 1-hour intervals from 1 to 12 hours, and 24 to 36 hours, as well as at 16, 48, 53, 60, 72, 82, 96 and 125 hours. Between measurements the OrganoPlate was placed back on the rocker platform to maintain flow. Fig. 4a-d depict arrays of images showing the fluorescence in the gel at each time-point for both FITC- and TRITC-dextran. Measurements for each compound were taken on a single OrganoPlate with 5 replicates per concentration. The staurosporine and aspirin studies were executed five and three times respectively on different days (see SI3 and SI4).

Fluorescence images of one single OrganoPlate depicted in the arrays of Fig. 4a-d and their quantification as depicted in Fig 4e, h show that barrier integrity was gradually diminished over time for all concentrations of staurosporine and for the

two highest concentrations of aspirin. Results can also be visualised by generating Kaplan-Meier plots for loss of barrier integrity, in which events are defined as the fluorescence ratio reaching 40% (Fig. 4f, i). This approach is particularly useful for less potent toxicants where EC50 determination suffers from a lack of data of high effect. Aspirin, which has a different mode of action involving tight junction disruption and proliferation inhibition, instead of apoptosis induction[20,21], causes much less barrier disruption at relevant concentration. The Kaplan-Meier curve, however, does show a highly significant trend of loss-of-barrier function at higher concentration ($P<0.0001$ for both curve difference and trend significance) (Fig 4i). An EC50 value was estimated for each time point by fitting the concentration response curve based on non-linear regression of the logarithm of the compound concentration versus the normalized fluorescence assuming a top and bottom plateau at 0 and 100% fluorescence. With increasing exposure times, a shift of EC50 towards lower compound concentrations was observed (Fig. 4g, j). The 95% confidence interval of the extracted EC50 values indicates robust data over the entire exposure time. EC50 values extracted at time points before the first event in the Kaplan Meier plots should be interpreted with caution as baseline fluorescence is likely to dominate the curve fitting rather than a biologically relevant signal.

SI4 shows an overlay of the EC50 curves for 5 independent experimental series of staurosporin (SI4a, b) and aspirin (SI4 c, d), based on both 150kDa FITC-dextran (SI4a, c) and 4.4kDa TRITC-dextran (SI4b, d) analysis. The high degree of similarity between the EC50 time curves for the full replicate series are a powerful illustration of the robustness of the method.

In parallel to fluorescence images, phase contrast pictures were taken at selected time points. An example of tube morphology as a response to 96 hours of staurosporine exposure is included in the supplementary information (SI5). Tubes are fully deteriorated for the highest concentration staurosporine and damages can be observed for exposure to 30µM staurosporine. For lower concentrations tubes appear intact, while fluorescence images show that barrier integrity is lost. This indicates that loss of barrier function at higher concentrations of staurosporin is primarily due to cell death. Dead cells are flushed away by the perfusion flow.

For comparison, a similar experiment in a conventional Transwell was performed, which revealed a lower sensitivity for barrier disruption compared to the OrganoPlate showing no significant difference between controls and staurosporine exposed wells after 4 hours (SI6), while a clear effect is already apparent in the OrganoPlate results. In addition to improved morphological maturity of the 3D perfused culture, the increased sensitivity of the model can be attributed to a decreased dead volume and higher surface to volume ratio of the microfluidic system as compared to Transwell systems. In a Transwell the FITC-dextran was strongly diluted in the large target volume when crossing the barrier. By contrast, in OrganoPlates the fluorescence is measured directly in the ECM after crossing the epithelial membrane. Since no dilution step is involved here, a much higher signal-to-noise ratio is obtained. Sensitivity of the microfluidic assay is such, that it can be used as a binary assay, in which the exposure time at which leakage is observed is indicative of the toxicity of the compound.

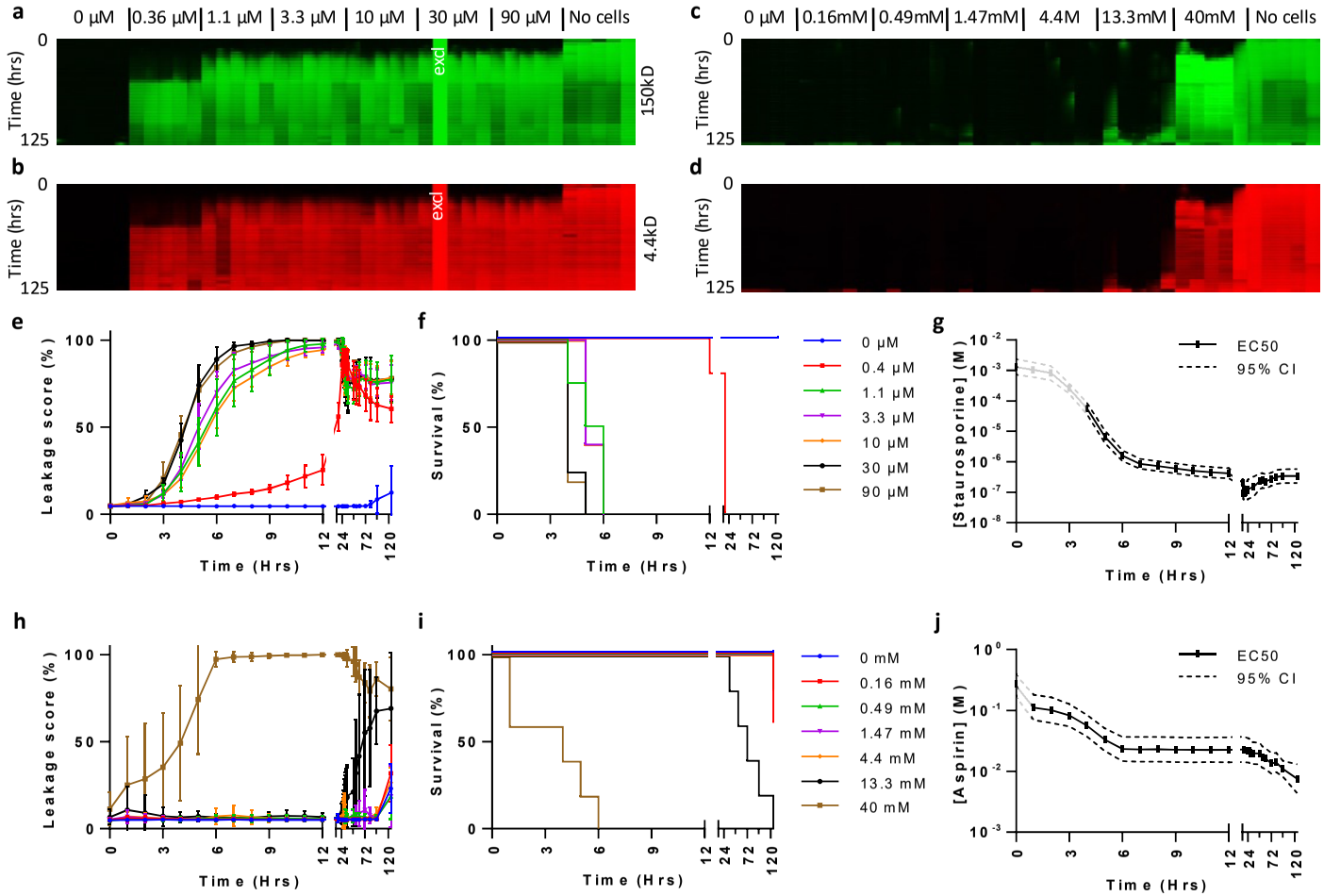
a
0 µM
0.36 µM
1.1 µM
3.3 µM
10 µM
30 µM
90 µM
No cells
Time (hrs)
0
125
excl
150kD
b
4.4kD
c
0 µM
0.16mM
0.49mM
1.47mM
4.4M
13.3mM
40mM
No cells
d
e
Leakage score (%)
Time (Hrs)
f
Survival (%)
0 µM
0.4 µM
1.1 µM
3.3 µM
10 µM
30 µM
90 µM
g
[Staurosporine] (M)
EC50
95% CI
h
i
0 mM
0.16 mM
0.49 mM
1.47 mM
4.4 mM
13.3 mM
40 mM
j
[Aspirin] (M)

Figure 4 | Drug induced loss of barrier integrity is observed over time in a concentration-dependent manner for staurosporine (a, b, e-g) and aspirin (c, d, h-j). (a-d) Array of fluorescence micrographs of the gel region showing distribution of the 150kDa FITC-Dextran (**a, c**) and 4.4kDa TRITC-Dextran (**b, d**) over time and for various compound concentrations; the loss of barrier integrity results in an increased fluorescent signal. Measurements are taken at 1-hour intervals up to 12 hours, at 16 hours, from 24 to 36 hours at 1 hour interval, and at 48, 53, 60, 72, 82, 96 and 125 hours. In between each interval, the OrganoPlate was placed back into the incubator on the interval rocker platform to maintain the perfusion flow. Five replicates of each concentration of a compound were measured on a single plate. One well was excluded from further data analysis, because of a pipetting error (marked with "excl" in white). **(e, h)** The progression of the loss of barrier function over time is plotted as the ratio between fluorescent signal in apical and basal regions for the various concentrations of staurosporine **(e)** and aspirin **(h)**, where the plotted line is the mean of 5 replicate exposures and error bars depict the standard deviation. **(f, i)** Kaplan-Meier curves were generated where survival was defined as showing a leakage score below 40%. Overlapping curves were shifted by 1% for clarity purposes. **(g, j)** EC50 values are plotted as a function of exposure time. EC50 values were obtained by fitting a concentration response curve at each time point based on non-linear regression of leakage scores using normalized response and standard slope and were plotted including 95% confidence interval (CI). EC50 values obtained from time points before the first event in the Kaplan-Meier plot, as indicated by grayed out line, should be interpreted with caution as the curve fit could be dominated by noise rather than biological effect. All shown graphs were derived from data acquired using 150kDa FITC dextran. Full replicate series were run for both staurosporine and aspirin on different days that are displayed in **SI3 and SI4**

Real-time measurement

Fig. 5 shows another concentration response experiment with staurosporine, but this time the OrganoPlate was continuously kept inside the microscope throughout the experiment. A conditioned high content imager was used to maintain appropriate CO_2, temperature and humidity. Flow was absent in this experiment, as the high content imager did not provide for rocking. As can be observed in fluorescent images and quantification thereof, vehicle control tubes started leaking after 6 to 8 hours of imaging. This can most likely be attributed to suboptimal conditions, including a lack of perfusion flow. Nevertheless, a clear concentration-response effect could be observed. An EC50-time curve was extracted and overlaid in red with the curve from the experiments with rocking in black (as shown previously in Fig. 4g) showing similar curves for up to 8 hours (Fig. 5c). The advantage of incubation in the microscope is that a higher time resolution can be obtained.

In the experimental series of Fig. 4, 5, SI3 and SI4 ten OrganoPlates were used, comprising a total of 357 gut tubes and 33 ECM-only negative controls in total. Two tubes were excluded because of pipetting errors and 26 because of insufficient barrier function after one hour, yielding 93% of leak tight tubes at the onset of drug exposure.

Discussion

In summary, we present a unique methodology for assessing the barrier integrity of 40 leak-tight, polarized epithelial gut tubes in parallel using high content imaging. It is for the first time that a comprehensive method is presented to interrogate perfused epithelia tubules that are exposed to an ECM. The system allows sensitive, real-time interrogation of compound effects on barrier integrity, yielding insight in both exposure concentration and exposure time effects. The method has been robustly demonstrated for over 350 gut tubes and over 20,000 datapoints, making this to our knowledge the largest published Organ-on-a-Chip dataset so far. The method can be applied to other epithelia as well as translated to disease models. The co-culture capabilities of the platform[9] can be explored to create complex tissue configurations, for example by incorporating mesenchymal and immune cells in the ECM adjacent to the epithelial tubes. The system outperforms classical techniques such as Transwell systems in terms of sensitivity, ease of use and

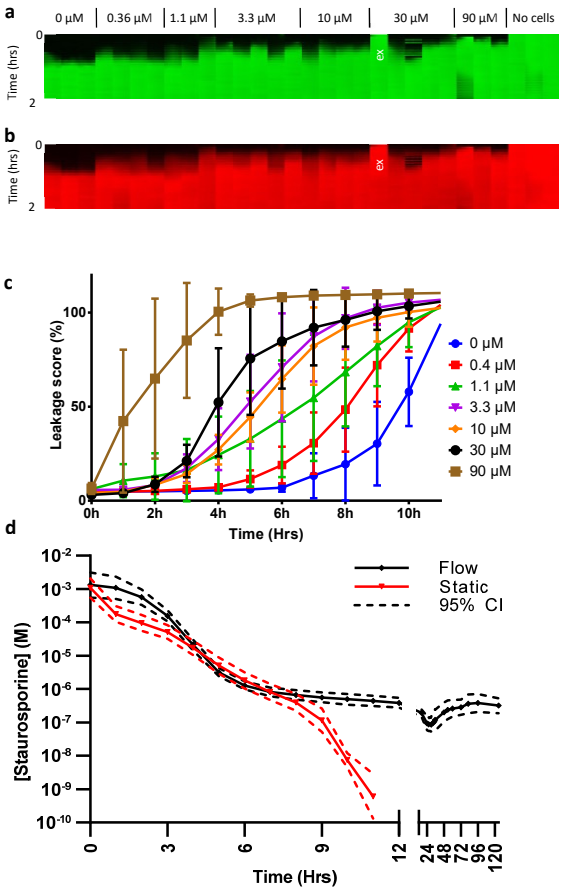

Figure 5 | Drug induced loss of barrier integrity as a function of staurosporine concentration measured in real-time. (a, b) Array of fluorescence micrographs of the gel region showing distribution of the 150kDa FITC-Dextran **(a)** and 4.4kDa TRITC-Dextran **(b)** over time and as a function of compound concentration; The OrganoPlate was continuously kept in an incubated automated microscope. Pictures were taken at 1 hour intervals. One data point was excluded for the fact that the tube appeared leaky at the first time point (marked with "excl" in white) **(c)** The progression of the loss of barrier function over time shows that untreated controls lose barrier integrity at 6-8 hours due to lack of flow. The plotted line is the mean of 3 to 5 replicate exposures and error bars depict the standard deviation. **(d)** EC50 values over time for real time measurement without flow and for measurement in intervals with flow induced between measurement (overlay with the graph of **Figure 4g)**. EC50 values with and without flow are similar for the initial 8 hours of measurement.

(multiplexed) readout flexibility, as well as reagent, cell and time consumption. More importantly, it allows for the first-time non-expert end-users to adopt organ-on-a-chip technology in their laboratories, without need for specific microfluidic skills or dedicated equipment.

Materials and Methods

Cell culture

The human colon adenocarcinoma cell line Caco-2 (86010202, Sigma-Aldrich) was cultured on T75 flasks in EMEM (#30-2003, ATCC), 10% FBS (#F4135, Sigma)), 1% NEAA (#11140-050, Life technologies) and 1% penicillin/streptomycin (Sigma #P4333). Caco-2 cells between passage 45 and 60 were used for all experiments.

OrganoPlate culture

OrganoPlate culture was performed using 3-lane OrganoPlates with 400 µm x 220 µm (w x h) channels (Mimetas BV, the Netherlands). Phaseguides had dimensions of 100 µm x 55 µm (w x h). Gel and perfusion channels have a length of 9 mm and 13 mm respectively. 2 µL of gel composed of 4 mg/mL Collagen I (AMSbio Cultrex 3D Collagen I Rat Tail, 5 mg/mL, Cat. 3447-020-01), 100 mM HEPES (Life Technologies, 15630-122) and 3.7 mg/mL $NaHCO_3$ (Sigma, Cat. S5761) was dispensed in the gel inlet and incubated 30-45 min at 37°C. Caco-2 cells were trypsinized using 0.5% trypsin in PBS/EDTA (Sigma, T3924) , aliquoted and pelleted (5 min, 100 x g). The cells were applied to the system by seeding 2 µl of 1 x 10^7 of cells/mL in the outlet of the top medium channel. Subsequently, the OrganoPlate was put on the side for 20 minutes to allow the cells to sediment against the ECM. This was followed by addition of 50 µL medium to the outlet of the top medium channel and the OrganoPlate was again incubated on the side for 3-4 hours at 37°C to complete cell attachment. After incubation, medium was added up to a total of 50 µL on both inlets and both outlets. The OrganoPlate was placed horizontally in the incubator (37°C 5% CO2) on an interval rocker switching between a +7° and -7° inclination every 8 minutes (Mimetas Rocker Mini) allowing bi-directional flow. Medium (50 µL each on inlet and outlet) was refreshed every 2 to 3 days.

Transwell culture

Caco-2 cells (60 x 10^3 cells/ cm^2) were seeded on Transwell inserts (24-well, Transwell, Costar #3470-Clear, 0.4 µM pore size) and cultured for 21 days in EMEM supplemented with 10% fetal calf serum (FCS), and penicillin/streptomycin (Sigma #P4333). Medium was refreshed every 2 to 3 days, both 100 µL on apical (insert) and 500 µL on basal side of the Transwell.

Immunohistochemistry

Caco-2 tubules were fixed with 3.7% formaldehyde (Sigma # 252549) in PBS (phosphate-buffered saline, Life tech # 20012068) for 15 min washed twice for 5 min with PBS and permeabilized with 0.3% Triton X-100 (Sigma # T8787) in PBS for 10 min. After washing with 4% FCS in PBS, cells were incubated with blocking solution (2% FCS, 2% bovine serum albumin (BSA) (Sigma # A2153), 0,1% Tween 20 (Sigma # P9416) in PBS) for 45 min. Subsequently, cells were incubated with primary antibodies for 60 min or at 4°C overnight, washed 3 times, incubated with secondary antibodies for 30 min and washed 3 times with 4% FCS in PBS. The following antibodies were used for immunohistochemistry: Rabbit a-ZO-1 (Invitrogen #617300, 1:125), Mouse a-acetylated tubulin (Sigma #T6793, 1:2000), Rabbit a-ErbB1 (Novusbio #NBP-1-51439, 1:200), Mouse a-MRP-2 (Santa cruz #SC-59608, 100 µg/ml, 1:10), Rabbit a-Glut-2 (Santa cruz #SC-9117, 200 µg/ml, 1:20), Mouse a-Ezrin (BD Transduction #610602, 1:50), Mouse a-ErbB2 (Thermo scientific #MS-229-P0, 200 µg/ml, 1:20), Rabbit a-Occludin (ThermoFisher #71-1500, 0.25 mg/ml, 1:100), Rabbit isotype (Life tech #86199), Mouse isotype (Life tech #86599), Goat isotype (Life tech #02-6202), Goat a-Rabbit AlexaFluor 488 (ThermoFisher, #A11008, 1:250), Goat a-Rabbit AlexaFluor 555 (LifeTechnologies, A21428, 1:250), Goat a-Mouse AlexaFluor 488 (LifeTechnologies, A11001, 1:250), Goat a-Mouse AlexaFluor 555 (LifeTechnologies, A21422, 1:250), Goat a-Mouse AlexaFluor 647 (LifeTechnologies, A-21236, 1:250), Donkey a-Rabbit AlexaFluor 647 (LifeTechnologies, A-31573, 1:250). After nuclear stain (DraQ5, Abcam # ab108410 or DAPI, H-1200, Vector Laboratories) cells were stored in PBS or Vectashield (H-1200, VectorLaboratories). All steps were performed at room temperature (RT). Cells were imaged with ImageXpress Micro XLS and Micro XLS-C High Content Imaging Systems (Molecular Devices, US) and SP5 laser point scanning confocal microscope (Leica).

Compound exposure

Caco-2 cells in OrganoPlates and Transwells were exposed to staurosporine or aspirin and barrier integrity was measured. Cells were exposed for 125 hours for interval measurements and for 24 hours for real-time measurements. Concentrations of aspirin were 0, 0.1, 0.33, 1.11, 3.67, 12.12, 40 mM (Sigma # A5376), and concentrations of staurosporine were 0, 0.4, 1.1, 3.3, 10, 30, 90 µM (Sigma # S4400). Aspirin was dissolved in medium. Staurosporine was dissolved in medium with 0.9% DMSO (Sigma, #D8418) for 90 µM and 0.3% for the other concentrations. Staurosporine preparations for the shorter term exposure also contain 3% tox medium (500 mL of MEMα (Sigma #M4526) with 6.25 mL of L-glutamine (Sigma #G7513), 6 mL Tox Supplement (Sigma #MTOXRTSUP).

Barrier integrity assay in OrganoPlate

Medium in the apical perfusion channel was replaced by medium containing 0.5 mg/mL FITC-dextran (150 kDa, Sigma # 46946) and TRITC-dextran (4.4 kDa, Sigma # T1037) and increasing concentrations of staurosporine or aspirin. Leakage of the fluorescent probe from the lumen of the tubular structure into the ECM compartment was automatically imaged using an ImageXpress XLS Micro High content imaging system at 37°C and 5% CO2. For long term exposure, imaging was performed at 1-hour intervals up to 12 hours, and from 24 to 36 hours, and at 16, 35, 36, 48, 53, 60, 72, 82, 96 and 125 hours. Between each interval, the OrganoPlate was placed back into the incubator on the interval rocker platform in order to maintain perfusion flow. For real time measurement, automatic imaging was performed every hour for 24 hours without removing the OrganoPlate from the HCI system. The ratio between the fluorescent signal in the basal and apical region of the tube was analyzed using FiJi[22].

Barrier integrity assay in Transwell

14-21h prior to start of the experiment, media was changed to Phenol-red free media (DMEM F12 (Gibco, 11039-021), 10% FBS HI (Sigma, F4135), 1% NEAA (Life tech, 11140050), 1% pen/strep (Sigma, P4333)). At the start of the compound exposure medium was replaced. 550 µL was added to the basolateral side, 250 µL of FITC-dextran solution (0.125mg/mL medium) mixed with the compound of choice was added to the apical side. At timepoints a 75 µL aliquot was collected from the basolateral side. 75 µL of fresh medium was added to the basolateral side

after the 2hr aspirin timepoint. The fluorescence intensity was measured with a multi-well plate fluorimeter (Fluoroskan Ascent FL, Thermo Fisher) with excitation at 485 nm and emission at 535 nm.

Statistics and data analysis

Barrier integrity assay images were analyzed using FiJi[22]. Fluorescence intensities where measured in the apical and basal regions of the tubes and the ratio between these was reported. Tubes that reached a 40% fluorescent intensity ratio at first hour of measurement were considered non-leak-tight and discarded. GraphPad Prism 6 (GraphPad Software Inc., La Jolla, CA) was used to generate Kaplan-Meier curves using the Survival Analysis – Survival Curve function defining an event as showing a basal to apical fluorescence intensity ratio over 40%. To prevent overlapping data, curves were nudged by 1 data point each for clarity. Curve difference was estimated using Log-rank (Mantel-Cox) test. Trend significance was evaluated using Log rank test.

Concentration response curves were fit using nonlinear regression of the logarithm of the compound concentration versus the normalized fluorescence assuming a top and bottom plateau at 0 and 100% and standard slope (hill slope=1). The estimated EC50 values and 95% confidence interval were plotted versus time.

Acknowledgements

We thank Prof. Dr. Hans Tanke for the use of the imaging facilities at the Department of Molecular Cell Biology, Leiden University Medical Center, and Joop Wiegant and Annelies van der Laan for their assistance. We thank Kitty Joore for generating artist impressions. E.N. and A.N. were supported by the EU Horizon 2020 program under project 674983 (Mimic) and 641639 (Biopol) respectively.

Competing financial interest

S.J.T., E.N., M.C.S., M.K.V., K.J.W., H.L.L., A.N., C.P.N., D.K., J.J., and P.V. are employees of MIMETAS BV, the Netherlands, that is marketing the OrganoPlate. P.V., J.J., T.H. and S.J.T. are shareholders of that same company. OrganoPlate® is a trademark of MIMETAS. A.B.R., S.K. and A.M. are employees of F. Hofmann-LaRoche Ltd and A.M. is a shareholder of F. Hofmann-LaRoche Ltd.

References

1. Pampaloni, F., Reynaud, E. G. & Stelzer, E. H. K. The third dimension bridges the gap between cell culture and live tissue. Nat. Rev. Mol. Cell Biol. 8, 839–45 (2007).
2. Weaver, V. M. et al. Reversion of the malignant phenotype of human breast cells in three-dimensional culture and in vivo by integrin blocking antibodies. J. Cell Biol. 137, 231–45 (1997).
3. van Duinen, V., Trietsch, S. J., Joore, J., Vulto, P. & Hankemeier, T. Microfluidic 3D cell culture: from tools to tissue models. Curr Opin Biotechnol 35, 118–126 (2015).
4. Tibbitt, M. W. & Anseth, K. S. Hydrogels as extracellular matrix mimics for 3D cell culture. Biotechnol. Bioeng. 103, 655–663 (2009).
5. Huh, D., Hamilton, G. A. & Ingber, D. E. From 3D cell culture to organs-on-chips. Trends Cell Biol. 21, 745–754 (2011).
6. Kim, H. J., Li, H., Collins, J. J. & Ingber, D. E. Contributions of microbiome and mechanical deformation to intestinal bacterial overgrowth and inflammation in a human gut-on-a-chip. Proc. Natl. Acad. Sci. 201522193 (2015). doi:10.1073/pnas.1522193112
7. Shah, P. et al. A microfluidics-based in vitro model of the gastrointestinal human–microbe interface. Nat. Commun. 7, 11535 (2016).
8. Junaid, A., Mashaghi, A., Hankemeier, T. & Vulto, P. An End-User Perspective on Organ-on-a-Chip: Assays and Usability Aspects. Curr. Opin. Biomed. Eng. (2017). doi:10.1016/j.cobme.2017.02.002
9. Trietsch, S. J., Israëls, G. D., Joore, J., Hankemeier, T. & Vulto, P. Microfluidic titer plate for stratified 3D cell culture. Lab Chip 13, 3548–3554 (2013).
10. Wevers, N. R. et al. High-throughput compound evaluation on 3D networks of neurons and glia in a microfluidic platform. Sci. Rep. 6, 38856 (2016).
11. Vulto, P. et al. Phaseguides: a paradigm shift in microfluidic priming and emptying. Lab Chip 11, 1596–602 (2011).
12. Giepmans, B. N. G. & van IJzendoorn, S. C. D. Epithelial cell–cell junctions and plasma membrane domains. Biochim. Biophys. Acta - Biomembr. 1788, 820–831 (2009).
13. Liang, T. W. et al. Characterization of huJAM: evidence for involvement in cell-cell contact and tight junction regulation. Am. J. Physiol. - Cell Physiol. 279, (2000).
14. Lever, J. E. Inducers of mammalian cell differentiation stimulate dome formation in a differentiated kidney epithelial cell line (MDCK). Proc. Natl. Acad. Sci. U. S. A. 76, 1323–1327 (1979).
15. Chantret, I., Barbat, A., Dussaulx, E., Brattain, M. G. & Zweibaum, A. Epithelial Polarity , Villin Expression , and Enterocytic Differentiation of Cultured Human Colon Carcinoma Cells : A Survey of Twenty Cell Lines Epithelial Polarity , Villin Expression , and Enterocytic Differentiation of Cultured Human Colon Carcinoma C. CANCER Res. 48, 1936–1942 (1988).
16. Pfister, A. B., Wood, R. C., Salas, P. J. I., Zea, D. L. & Ramsauer, V. P. Early response to ErbB2 over-expression in polarized Caco-2 cells involves partial segregation from ErbB3

by relocalization to the apical surface and initiation of survival signaling. J. Cell. Biochem. 111, 643–52 (2010).
17. Johnson, L. R. Physiology of the gastrointestinal tract. (Academic Press, 2012).
18. Belmokhtar, C. A., Hillion, J. & Ségal-Bendirdjian, E. Staurosporine induces apoptosis through both caspase-dependent and caspase-independent mechanisms. Oncogene 20, 3354–3362 (2001).
19. Oshima, T., Miwa, H. & Joh, T. Aspirin induces gastric epithelial barrier dysfunction by activating p38 MAPK via claudin-7. Am J Physiol Cell Physiol 295, C800-806 (2008).
20. Ricchi, P. et al. Effect of aspirin on cell proliferation and differentiation of colon adenocarcinoma Caco-2 cells. Int. J. Cancer 73, 880–4 (1997).
21. Matsui, H. et al. The pathophysiology of non-steroidal anti-inflammatory drug (NSAID)-induced mucosal injuries in stomach and small intestine. J. Clin. Biochem. Nutr. 48, 107–11 (2011).
22. Schindelin, J. et al. Fiji: an open-source platform for biological-image analysis. Nat. Methods 9, 676–82 (2012).

Supplementary information

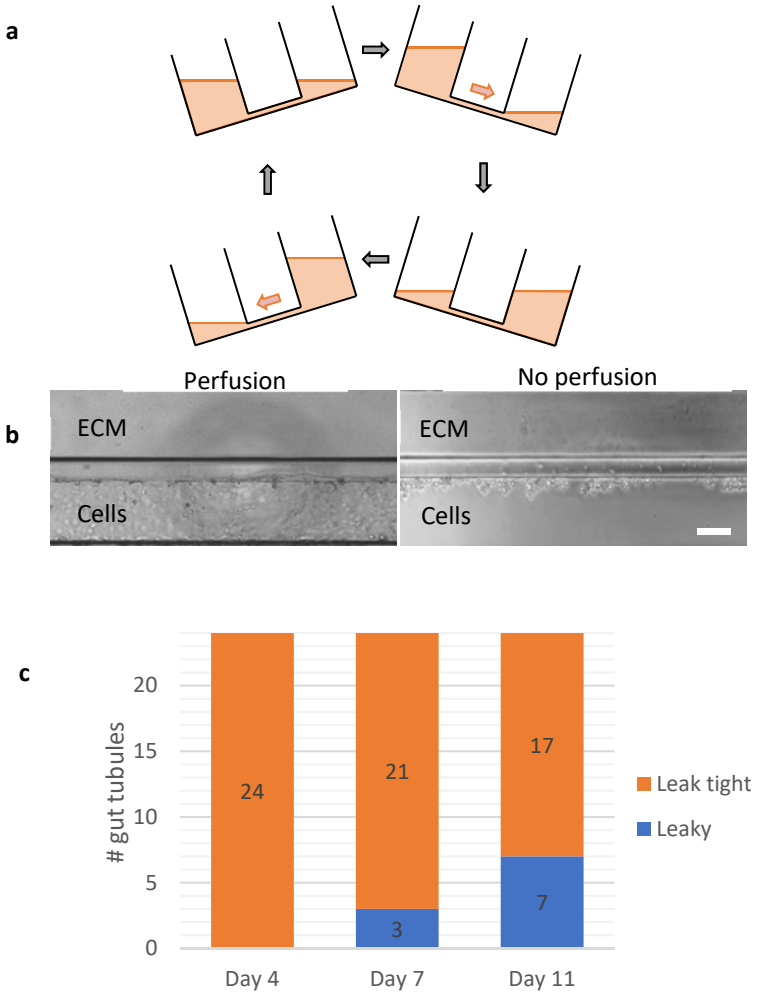

SI1 | Flow induction in OrganoPlate. (a) Flow is induced by leveling between two reservoirs that are connected by the perfusion channel. By placing the plate under an angle on an interval rocker that inverts the angle at regular intervals, a continuous bi-directional flow through the perfusion channel is induced. **(b)** Influence of flow on tube formation: A confluent tube of Caco-2 cells is formed within three days when perfused (left), while few cells survive culture without perfusion (right). Scale bars are 100µm. **(c)** Number of leak tight and leaky tubes in a single experimental run. Fluorescence intensity in the gel is measured and normalized to the fluorescence level in the tube channel. Upon crossing a threshold value of 0.4, a tube is considered leaky. At day 4 all tubes are leak tight, while at day 11 approximately 29% of tubes are leaking.

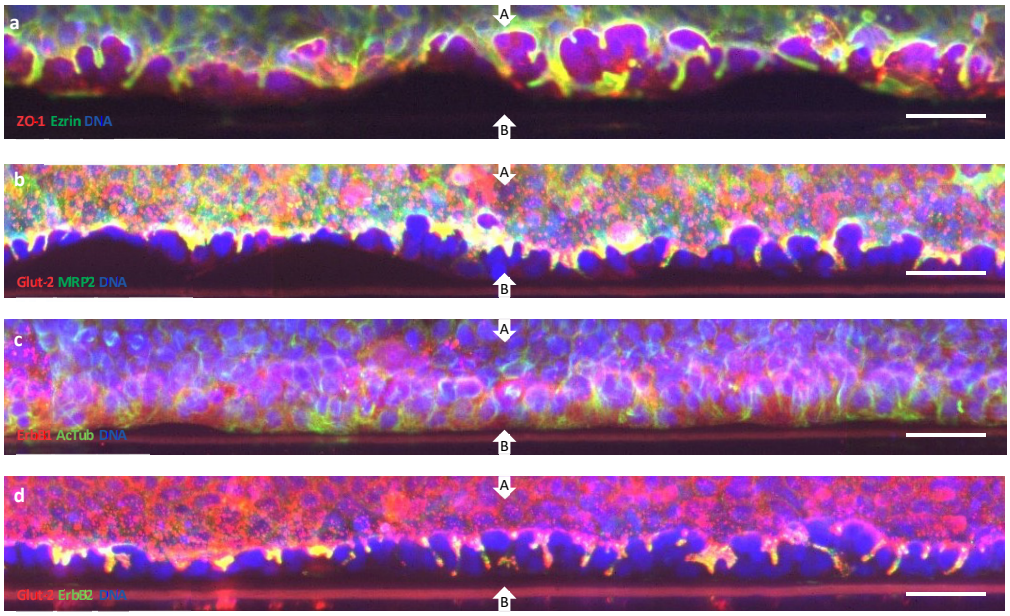

SI2 | Tubule characterization by immunofluorescent staining. Z-slices at higher magnification of confocal fluorescence micrographs of tubes from **fig. (2)** focusing on barrier morphology against ECM at approx. 50 µm above the bottom of the tube. An optical slice of the cells attached to the ECM is shown with white arrows indicating the apical (A) and basal (B) sides. The tube is stained for tight junctions (ZO-1 in red) and brush borders (Ezrin in green) showing apical positioning of Ezrin indicating polarization of the tube and invaginations expressing transport proteins. **(b)** expression of glucose and MRP2 transporters respectively stained with Glut-2 in red and MRP2 stain in green. Both stains clearly stain the apical side of the tube. **(c)** ErbB1 (red) and acetylated tubulin (green) expression. **(d)** Co-staining of Glut-2 transporter (red) and ErbB2 receptor (green); ErbB2 is primarily expressed pericellularly (here appearing as yellow). All tubes are fixated after four days in culture. Scale bars in white are 50µm.

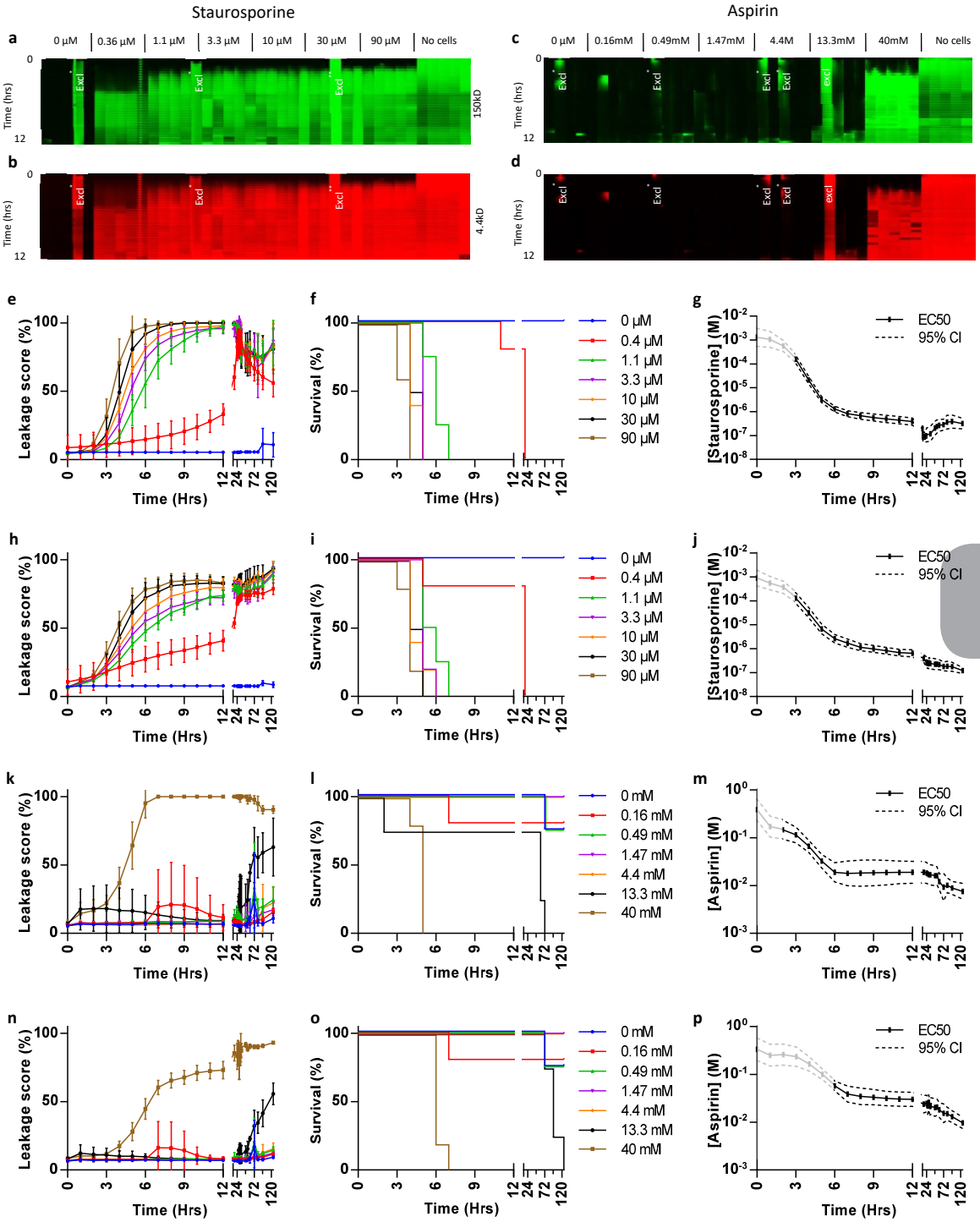
Staurosporine
Aspirin
a
b
c
d
0 µM
0.36 µM
1.1 µM
3.3 µM
10 µM
30 µM
90 µM
No cells
0.16mM
0.49mM
1.47mM
4.4M
13.3mM
40mM
Excl
Time (hrs)
150kD
4.4kD
e
f
g
h
i
j
k
l
m
n
o
p
Leakage score (%)
Survival (%)
[Staurosporine] (M)
[Aspirin] (M)
Time (Hrs)
EC50
95% CI
0 µM
0.4 µM
1.1 µM
3.3 µM
10 µM
30 µM
90 µM
0 mM
0.16 mM
0.49 mM
1.47 mM
4.4 mM
13.3 mM
40 mM

SI3 | Full replicate of the experimental series in Figure 4 in which loss of barrier integrity is observed over time in a concentration-dependent manner for staurosporine (a, b, e-j) and aspirin (c, d, k-p). (a-d) Array of fluorescence micrographs of the gel region showing distribution of the 150kDa FITC-Dextran **(a, c)** and 4.4kDa TRITC-Dextran **(b, d)** over time and as a function of compound concentration; the loss of barrier integrity is shown by an increased fluorescent signal. Measurements are taken at 1-hour intervals up to 12 hours, at 16 hours, from 24 to 36 hours at 1 hour interval, and at 48, 53, 60, 72, 82, 96 and 125 hours. In between each interval, the OrganoPlate was placed back into the incubator on the interval rocker platform. Five replicates of each concentration of a compound were measured on one single plate. Seven experimental runs were excluded from further data analysis, because the tubes appeared leaky at the first measurement (indicated with "Excl*") and one run was excluded because of a pipetting error (indicated with "Excl**"). **(e, h, k, n)** The progression of the loss of barrier function over time is plotted as the ratio between fluorescent signal in apical and basal regions for the various concentrations of staurosporine **(e, h)** and aspirin **(h, n)**; **(e, k)** show barrier integrity measurement using 150 kDa FITC dextran as a leakage marker, while **(h, n)** show barrier integrity measurement using 4.4 kDa TRITC-dextran as a leakage marker. The plotted line is the mean of 5 replicate exposures minus excluded datapoints and error bars depict the standard deviation **(f, i, l, o)** Kaplan-Meier curves were generated where survival was defined as showing a leakage score below 40%. Overlapping curves were shifted by 1% for clarity purposes. **(g, j, m, p)** EC50 values as a function of exposure time. EC50 values where obtained by fitting a concentration response curve at each time point based on non-linear regression of normalized leakage scores using standard slope. EC50 values obtained from time points before the first event in the Kaplan-Meier plot, as indicated by grayed out line, should be interpreted with caution as the curve fit could be dominated by noise rather than biological effect.

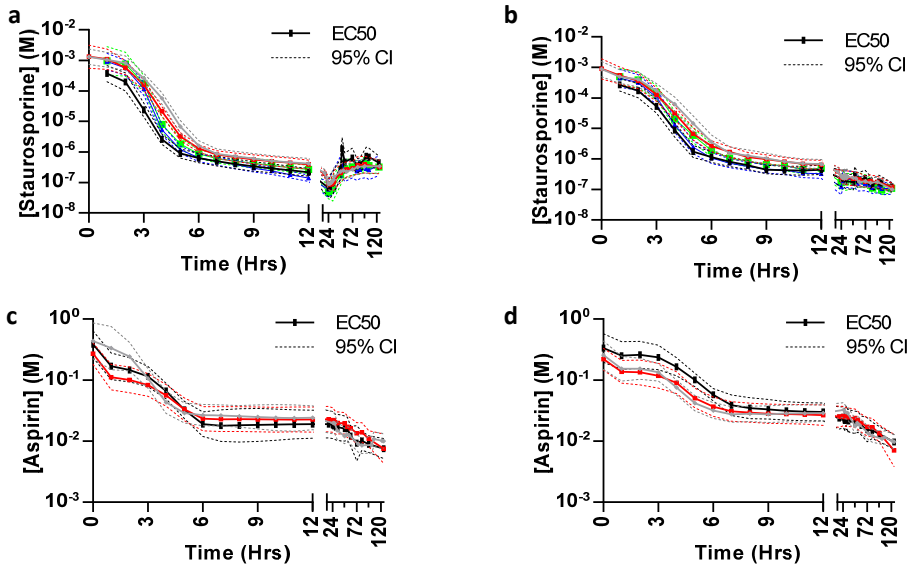

SI4 | Overlay of EC50 time curves of staurosporine and aspirin. The robustness of the assay was evaluated by multiple replicate series of the experimentals serie depicted in figure 4 and SI3 executed on different days. The EC50 time curves were generated for 5 independent staurosporine studies (**a, b**) and 3 independent aspirin studies (**c, d**). Figures **a, c** show results for 150kDa FITC-Dextran and figures **b, d** show results for 4.4kDa TRITC-Dextran. Independent experimental series show comparable results, confirming the robustness of the assays. The EC50 curves represent a total of 330 Caco tubes and over 18,000 datapoints.

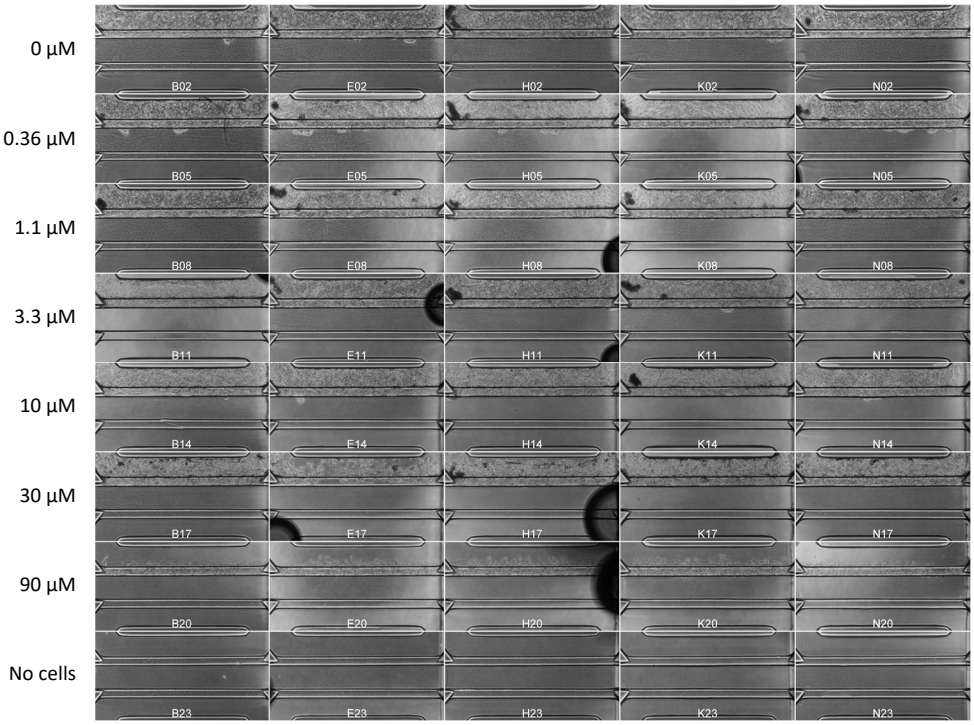

SI5 | Phase contrast images of Caco-2 tubes after 96 hours of staurosporine exposure. Even though all concentration already show leakage at this time point, a confluent monolayer is still observed at all but the highest concentration. At 90 µM tubes have fully deteriorated. Dead cells detach and are flushed away by the perfusion flow.

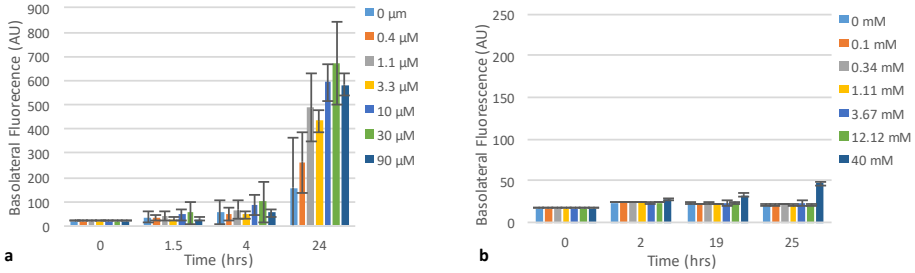

SI6 | Barrier integrity on Caco-layers in conventional Transwell systems exposed to (a) staurosporine and (b) aspirin. Caco-2 cells were seeded at a density of $60x10^3$ cells/cm^2 on 6.5 mm polyester Transwell inserts with 0.4µm pores. Media was replaced three times per week (DMEM, 10% FCS, 1% NEAA, glutamax, p/s) for three weeks. After three weeks, the apical medium was replaced with 250 µL of medium containing a fluorescent probe (150kD FITC dextran) and staurosporine **(a)** or aspirin **(b)** at varying concentrations. The basolateral media was replaced with 550µL fresh medium. At various time points, 75µL basolateral medium was sampled to perform fluorescence measurements using a Fluoroskan FL plate reader. 75µL fresh medium was added after the aspirin 2hr timepoint to maintain sufficient sample for the remaining sampling time points. Fresh medium was used for 0 hour measurements. Four replicas were used for aspirin at 0 to 0.34 mM and three replicates for the remaining concentrations. For staurosporine 4, 3, 3, 3, 4, 3, and 4 replicates were performed at 0, 0.4, 1.1, 3.3, 10, 30 and 90µM respectively.